

zation from benzene gave 25.6 mg of crystals, mp 159–163 °C.

Anal. Calcd for $C_{17}H_{16}O_3$: C, 76.10; H, 6.01. Found: C, 77.56, 77.34; H, 6.38, 6.21.

The infrared spectrum of the product shows absorption at 3400 (OH st), 2600–2700 (COOH), and 1700 cm^{-1} (C=O).

1-Keto[2.2]paracyclophane from 1-Hydroxy[2.2]paracyclophane-1-carboxylic Acid. A mixture of 130 mg of 1-hydroxy-[2.2]paracyclophane-1-carboxylic acid, 2.4 ml of acetone, 2.4 ml of acetic acid, 0.6 ml of water, and 600 mg of powdered sodium periodate was stirred at 45 °C for 20 h, concentrated in a stream of nitrogen, treated with cold water, and filtered to give 80.7 mg (75%) of 1-keto-[2.2]paracyclophane.

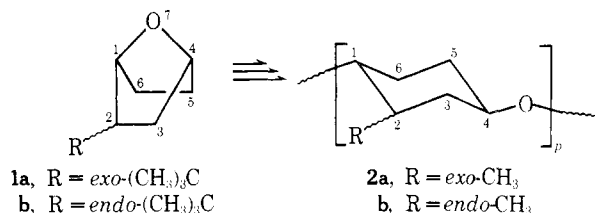
Kinetic Study of Polymerization of 2-*tert*-Butyl-7-oxabicyclo[2.2.1]heptane

Takeo Saegusa,* Masatoshi Motoi, and Hiroshi Suda

Department of Synthetic Chemistry, Faculty of Engineering, Kyoto University, Kyoto, Japan. Received December 22, 1975

ABSTRACT: Kinetics of the polymerizations of *exo*- and *endo*-2-*tert*-butyl-7-oxabicyclo[2.2.1]heptanes (**1a** and **1b**) were studied by means of the Phenoxyl End-Capping method. The propagation rate constants and the activation parameters were determined. The reactivities of **1a** and **1b** were discussed and compared with those of the methyl homologues.

This paper describes a kinetic study of the cationic polymerizations of *exo*- (**1a**) and *endo*-2-*tert*-butyl-7-oxabicyclo[2.2.1]heptanes (**1b**) in CH_2Cl_2 with BF_3 -tetrahydrofuran (THF) complex–epichlorohydrin (ECH) system as initiator. As reported in our preceding paper,¹ propagation in the polymerization of *tert*-butyl monomers proceeds via an SN_2 reaction between the monomer and the propagating oxonium ion. Polymerizations of the *tert*-butyl monomers suffered from fairly rapid termination to generate olefinic ends. Such termination was not significant in the polymerizations of the methyl homologues. In our previous papers,^{2,3} the polymerization reactivities of **2a** and **2b** (the methyl homologues) were



also examined. The effects of size and geometric position (*exo* or *endo*) of the alkyl substituent of bicyclic ether monomer on the polymerization reactivity are of great interest. In the present paper, the polymerization reactivities of **1a** and **1b** are examined and compared with those of the methyl homologues.

Solution polymerizations of **1a** and **1b** were carried out in CH_2Cl_2 at temperatures in the range between –40 and 0 °C. Figures 1 and 2 show the time–[P*] (concentration of propagating species) profiles of their polymerizations, in which [P*] was determined by the “Phenoxyl End-Capping” method.⁴ It is indicated that the decrease of [P*] becomes pronounced at higher reaction temperatures. This observation is in agreement with the result of our previous study in which the olefin contents of the product polymers prepared at various temperatures were analyzed by ir spectroscopy.¹

The polymer yield was low as shown in time–conversion curves (Figures 3 and 4). The kinetic analysis was performed in an early stage of polymerization, because the concentration of olefinic linkages formed by termination became significant

References and Notes

- (1) Contribution No. 2333.
- (2) D. J. Cram and R. C. Helgeson, *J. Am. Chem. Soc.*, **88**, 3515 (1966).
- (3) In recent inhalation studies at our Haskell Laboratory for Toxicology and Industrial Medicine, hexamethylphosphoramide has been found to be carcinogenic in rats. Accordingly, any work with hexamethylphosphoramide should be carried out in an efficient hood to avoid inhalation of vapors. Since it is absorbed by the skin, care should be taken to avoid contact with hexamethylphosphoramide.
- (4) E. Hedaya and L. M. Kyle, *J. Org. Chem.*, **32**, 197 (1967).
- (5) E. Vedejs, *J. Am. Chem. Soc.*, **96**, 5944 (1974).

as polymerization progressed. This disturbed the determination of [P*] by uv absorption of phenoxyl group at 272 nm in the “Phenoxyl End-Capping” method. As shown in the spectra of the polymers obtained under varying conditions (Figure 5), the absorption curve for the phenoxyl group was deformed as polymerization proceeded, especially at elevated temperatures. The points in parentheses in Figures 1 and 2 were obtained on the basis of the deformed uv spectra. Therefore, these points were not used in the subsequent kinetic analysis. The formation of olefinic linkage was observed at similar concentrations when the polymerization mixture was not treated with sodium phenoxide. Thus, the olefinic group at the polymer end is not generated by “Phenoxyl End-Capping” reaction.

The rate of monomer consumption in the propagation step is formulated according to the SN_2 reaction between the propagating species and the monomer:

$$-d[M]/dt = k_p [P^*][M] \quad (1)$$

where [M] and k_p are the monomer concentration and the propagation rate constant, and [P*] has already been described above. In the cases of **2a** and **2b**, the propagation step was established to be irreversible by a depolymerization experiment in which the purified polymers of **2a** and **2b** were treated with $Et_3O^+SbCl_6^-$ at –20 °C for 96 h to generate no monomer by gas chromatographic analysis.^{2,3} In poly(**1a**) and poly(**1b**), the depolymerization by the cyclization of the monomeric unit of polymer into the monomer is also deemed impossible. Therefore, the propagations of **1a** and **1b** are considered to be irreversible processes. Integration of eq 1 between times t_1 and t_2 gives eq 2, where $[M]_{t_1}$ and $[M]_{t_2}$ are monomer concentrations at times t_1 and t_2 . The integrated value of [P*] could be obtained by graphical integration of the time–[P*] curve, and the monomer concentrations were calculated from the amount of polymer produced. A plot of $\int_{t_1}^{t_2} [P^*] dt$ vs. $\ln([M]_{t_1}/[M]_{t_2})$ gave a linear relationship as exemplified in Figures 6 and 7. The k_p value was obtained from the slope of the line. Arrhenius plots of the k_p values gave the activation parameters (Figure 8). In Table I, the k_p 's and

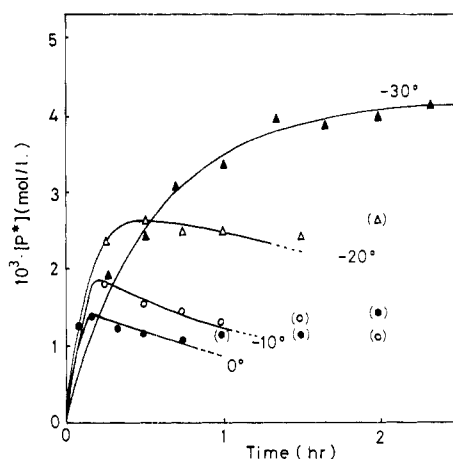


Figure 1. Time- $[P^*]$ curve in polymerization of **1a** by BF_3 -ECH system in CH_2Cl_2 : $[M]_0$, 1.95 M; $[\text{BF}_3\cdot\text{THF}]_0$, 0.0382 M; $[\text{ECH}]_0$, 0.0408 M. The points in parentheses were obtained on the basis of uv spectra which were deformed by the presence of olefinic bond at polymer end.

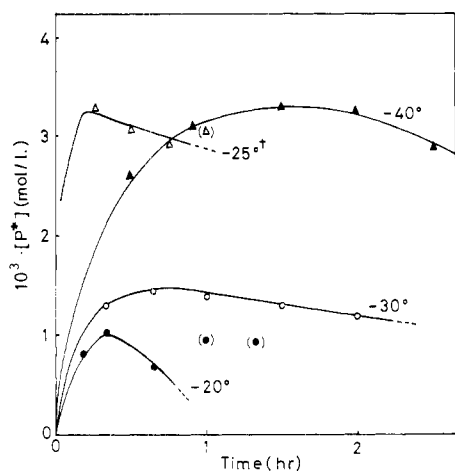


Figure 2. Time- $[P^*]$ curve in polymerization of **1b** by BF_3 -ECH system in CH_2Cl_2 : $[M]_0$, 1.85 M; $[\text{BF}_3\cdot\text{THF}]_0$, 0.0385 M; $[\text{ECH}]_0$, 0.0372 M. The points in parentheses were obtained on the basis of uv spectra which were deformed by the presence of olefinic bond at polymer end.

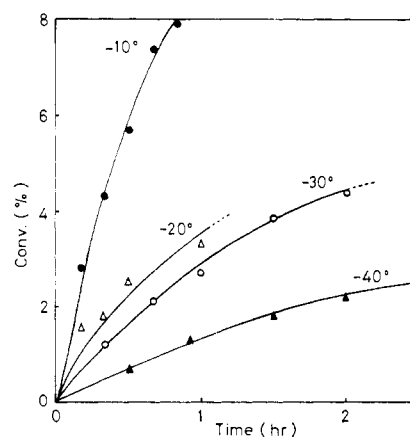


Figure 4. Time-conversion curve in the polymerization of **1b** by BF_3 -ECH system in CH_2Cl_2 : $[M]_0$, 1.85 M; $[\text{BF}_3\cdot\text{THF}]_0$, 0.0385 M; $[\text{ECH}]_0$, 0.0372 M.

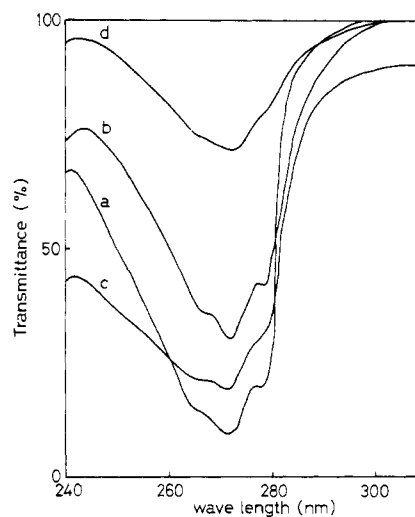


Figure 5. Uv spectra of phenoxyl end-capped polymer of **1a** in the BF_3 -ECH-catalyzed polymerization in CH_2Cl_2 : (a) at -30°C , after 140 min; (b) -20°C , 45 min; (c) -20°C , 90 min; (d) -10°C , 30 min.

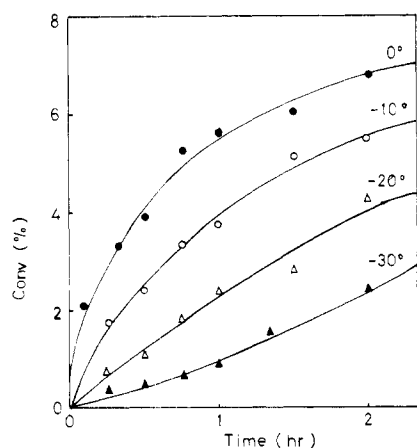


Figure 3. Time-conversion curve in the polymerization of **1a** by BF_3 -ECH system in CH_2Cl_2 : $[M]_0$, 1.95 M; $[\text{BF}_3\cdot\text{THF}]_0$, 0.0382 M; $[\text{ECH}]_0$, 0.0408 M.

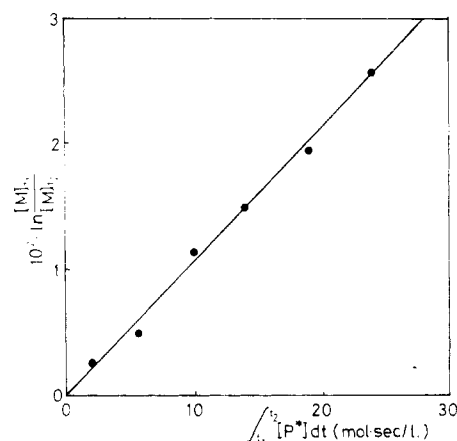


Figure 6. $\int_{t_1}^{t_2} [P^*] dt$ vs. $\ln([M]_{t_1}/[M]_{t_2})$ plot for the polymerization of **1a** by BF_3 -ECH at -30°C : solution polymerization in CH_2Cl_2 ; $t_1 = 30$ min.

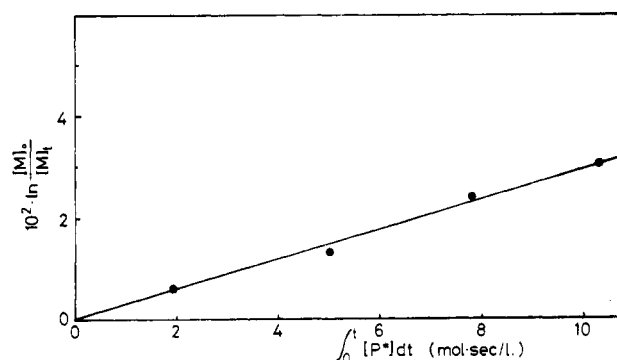


Figure 7. $\int_0^t [P^*] dt$ vs. $\ln ([M]_0/[M]_t)$ plot for the polymerization of **1b** by $\text{BF}_3\text{-ECH}$ at -30°C ; polymerization in CH_2Cl_2 .

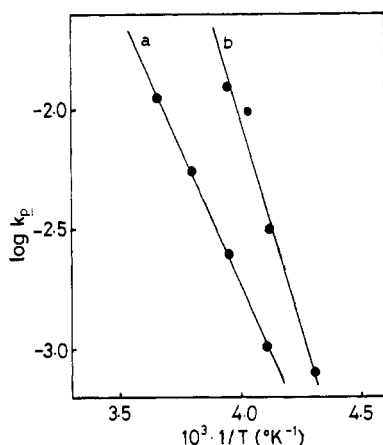


Figure 8. Arrhenius plots of propagation rate constants of the polymerizations of **1a** and **1b** by $\text{BF}_3\text{-ECH}$ in CH_2Cl_2 : (a) **1a**; (b) **1b**.

the activation parameters of **1a** and **1b** are summarized together with those of **2a** and **2b**. It is seen that the k_p values for *tert*-butyl and methyl homologues of the same structures (the comparisons of two sets of monomers **1a-2a** and **1b-2b**) are quite similar to each other. In the comparison between *exo* and *endo* monomers, i.e., **1a-1b** and **2a-2b**, the *endo* monomer is more reactive than *exo* monomer. The strain due to repulsions between the *endo* alkyl group and hydrogen atoms at C-3 and C-6 in the propagating bicyclic oxonium may contribute to an increase in the ring-opening reactivities of bicyclic oxoniums of **1b** and **2b**. However, the results of kinetic analysis in the present study indicate that the effect of frequency factor upon k_p predominates over that of the activation energy. The higher value of k_p of **1b** in comparison with **1a** is ascribed to a higher

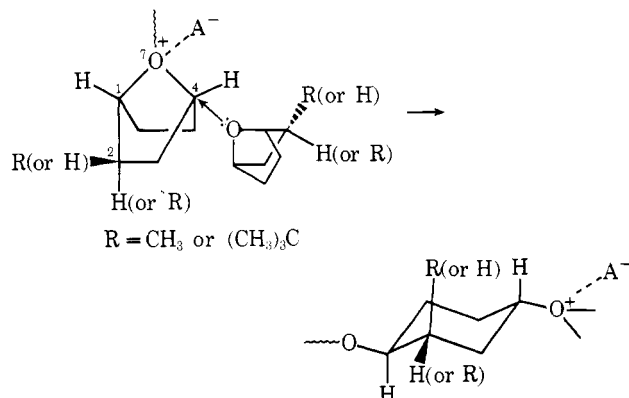


Table I
Comparison of Reactivities of 2-Alkyl-7-oxabicyclo[2.2.1]-heptanes for $\text{BF}_3\text{-ECH}$ -Catalyzed Polymerization^a

	Temp ^b °C	1a <i>exo-tert</i> - butyl	1b <i>endo-tert</i> - butyl	2a ^c <i>exo</i> - methyl	2b ^d <i>endo</i> - methyl
$10^3 k_p$, l./ (mol s)	-40		0.82	0.18	0.85
	-30	1.0	2.9	0.87	4.0
	-25		9.9		
	-20	2.5	13	2.6	8.4
	-10	5.7		9.4	26.7
	0	11.5			
ΔE_p^\ddagger , kcal/ mol		11.1	16.6	15.3	13.8
$10^6 A_p^\ddagger$, l./ (mol s)		5	3×10^6	4×10^4	7×10^3
ΔH_p^\ddagger , kcal/ mol		10.2	15.5	15.2	13.2
ΔS_p^\ddagger , eu		-30.0	-6.0	-15.2	-10.0

^a Solution polymerization in CH_2Cl_2 . Conditions are given in Figures 1 and 2. ^b The accuracy of temperature was within $\pm 0.5^\circ\text{C}$. ^c From ref 2. ^d From ref 3.

(more favorable) frequency factor. The activation energy for propagation of **1b** is even higher (less favorable) than that for **1a**. A lower value of frequency factor (a more negative value of ΔS_p^\ddagger) for **1a** may be explained by assuming decreased solvation due to increased steric hindrance by the *exo-tert*-butyl group in the ground state. The entropy gained by desolvation of the transition state is smaller in the propagation of **1a** than in the propagation of **1b**, and, consequently, the frequency factor of **1a** becomes smaller. A higher value of activation energy for **1b** may be due in part to the higher energy required for desolvation.

$$\ln [M]_{t_1}/[M]_{t_2} = k_p \int_{t_1}^{t_2} [P^*] dt \quad (2)$$

Experimental Section

Materials. *exo*- and *endo*-2-*tert*-butyl-7-oxabicyclo[2.2.1]heptanes (**1a** and **1b**) were prepared according to our previous paper.¹ They were distilled over Na wire prior to use. Purities of **1a** and **1b** by gas chromatographic analysis were above 99.9 and 98.0%, respectively. $\text{BF}_3\text{-THF}$ complex (initiator) was prepared by passing BF_3 gas into THF as previously reported,⁵ bp $87.5\text{--}87.8^\circ\text{C}$ (11 mm) (lit.⁵ 79.0°C (7.2 mm)). ECH (promotor) and CH_2Cl_2 (solvent) were purified by the usual methods.

Polymerization Procedure. Polymerization was carried out under dry nitrogen. A mixture of monomer (0.4–0.5 ml) and ECH solution in CH_2Cl_2 was placed at a desired temperature in a tube to which a solution of $\text{BF}_3\text{-THF}$ complex in CH_2Cl_2 was added. After polymerization was complete, a solution of sodium phenoxide in THF was added to the system. The mixture was extracted twice with CH_2Cl_2 . The extracts were combined and dried over anhydrous K_2CO_3 . The CH_2Cl_2 solution was filtered, diluted to 10 ml, and subjected to analysis by uv spectroscopy at λ_{max} 272 nm (ϵ , $1.93 \times 10^3 \text{ l./mol cm}$). The solution was evaporated, and the residue was dried in vacuo and weighed to determine the yield of polymer.

References and Notes

- (1) T. Saegusa, M. Motoi, and H. Suda, in press.
- (2) T. Saegusa, S. Matsumoto, M. Motoi, and H. Fujii, *Macromolecules*, **5**, 236 (1972).
- (3) T. Saegusa, M. Motoi, S. Matsumoto, and H. Fujii, *Macromolecules*, **5**, 815 (1972).
- (4) T. Saegusa and S. Matsumoto, *J. Polym. Sci., Part A-1*, **6**, 1559 (1968).
- (5) R. C. Ostoff, C. A. Brocon, and J. A. Howkins, *J. Am. Chem. Soc.*, **73**, 5480 (1951).